IEEE Access
Multidisciplinary | Rapid Review | Open Access Journal

Received May 21, 2020, accepted June 6, 2020, date of publication June 9, 2020, date of current version June 19, 2020.

Digital Object Identifier 10.1109/ACCESS.2020.3001135

Finite Blocklength Error Probability Distribution for Designing Ultra Reliable Low Latency Systems

ONEL L. ALCARAZ LÓPEZ [1], (Member, IEEE), HIRLEY ALVES [1], (Member, IEEE), RICHARD DEMO SOUZA [2], (Senior Member, IEEE), AND MATTI LATVA-AHO [1], (Senior Member, IEEE)

[1]Centre for Wireless Communications, University of Oulu, 90014 Oulu, Finland
[2]Department of Electrical and Electronics Engineering, Federal University of Santa Catarina, Florianópolis 88040-900, Brazil

Corresponding author: Onel L. Alcaraz López (onel.alcarazlopez@oulu.fi)

This work was supported in part by the Academy of Finland 6Genesis Flagship under Grant 318927, Grant 307492, and Grant 319008, in part by the Finnish Foundation for Technology Promotion, through PrInt Coordination for the Improvement of Higher Education Personnel (CAPES), Federal University of Santa Catarina (UFSC) Automation 4.0, and in part by the Brazilian National Council for Scientific and Technological Development (CNPq), Brazil.

ABSTRACT Future wireless systems are envisioned to support completely new use cases with extremely stringent requirements on both latency and reliability, e.g., Ultra-Reliable Low-Latency Communication. However, guaranteeing truly reliable services is quite challenging, much more under strict latency constraints. Notice that when it comes to reliability, the traditional approaches relying on average performance figures do not provide sufficient reliability guarantees. Instead, analyses/designs based on risk measures are more useful since they offer a more fine-grained probabilistic information of the system reliability. In this paper, we depart from novel information theory results on finite-blocklength (FB) coding, which characterize the error-latency trade-off under strict delay constraints, to highlight that the FB error probability is in fact a random variable in fading scenarios. Then, we provide accurate analytical approximations for the FB error probability distribution. This allows us to evaluate some well-known risk measures and, based on them, quantify the system reliability under strict latency constraints from different standpoints. We validate our results via simulation and provide numerical examples that illustrate, for instance, that two systems performing similar in terms of average reliability, may offer services with different risk perceptions.

INDEX TERMS Ultra-reliability, finite blocklength, error probability distribution, risk measures.

I. INTRODUCTION

The advent of fifth generation (5G) of wireless systems opens up new possibilities and gives rise to new use cases with stringent delay and reliability requirements, e.g., Ultra Reliable Low Latency Communication paradigm (URLLC), as in mission critical communications and coordination among vehicles. For instance, 1ms of user-plane latency is targeted in the ''general URLLC case'' when transmitting a message payload of 32 bytes with average reliability of $1 - 10^{-5}$ [1]. To sustain such low latency links, messages have to be short, and asymptotic performance metrics like Shannon capacity, and its extension to nonergodic channels, are no longer necessarily appropriate [2]. Recent results in the field of finite-blocklength (FB) information theory deal with a more suitable metric, which is the maximum achievable rate at a given blocklength and error probability [3], [4]. This metric is proportional to the largest amount of information nats k that can be mapped into a packet of n channel uses, under the constraint that the information nats are recovered at the receiver with success probability no smaller than $1-\epsilon$. For the sake of reliability analysis we can alternatively characterize the error probability ϵ as a function of k, n, and the Signal-to-Interference-plus-Noise Ratio (SINR).[1] Different from the asymptotic results, an error may occur with a given probability in the FB case, even when the SINR is large.

A. MOTIVATION

So far, the design and analysis of URLLC systems, under different setups and considering diverse goals, is based on *average* reliability formulations, e.g. [6]–[10]. Under the FB assumption, the related works reach at different conclusions than they would if the asymptotic formulation was utilized,

The associate editor coordinating the review of this manuscript and approving it for publication was Li Zhang.

[1]Readers can refer to [5] for a review of some of the most promising code constructions targeting the short block regime.

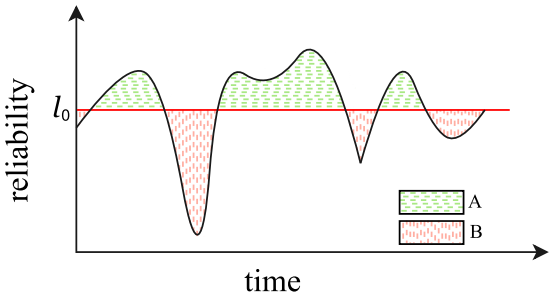

FIGURE 1. Reliability behavior as a function of time. A and B denote the regions in which the reliability is above and below the average l_0, respectively.

reinforcing the significance of the new information theoretic results introduced in [2]–[4]. This is also the case of SINR meta-distribution approaches for large-scale networks, which focus on per-link *average* reliability instead of the usual average network reliability as in [11], [12]. However, as discussed in [13], URLLC mandates a departure from typical network design approaches, which rely on average quantities, to approaches based on risk metrics. Following this path, a distributed risk-sensitive reinforcement learning-based framework was recently proposed in [14] to jointly optimize the beamwidth and transmit power while providing gigabit wireless access with reliable communication in 5G millimeter-wave (mmWave) networks.

Figure 1 shows a typical system behavior where l_0 could be the average system reliability over time. Notice that at a given time instant the transmission success is binary: the transmission may or may not be successful only. Ultimately, this depends on the system instantaneous characteristics, e.g., SINR, modulation, error correcting codes, etc, and the success probability can be written as a function of them. The time variability in Fig. 1 implies a variability in the system instantaneous characteristics, hence, the reliability rather than a binary parameter it is equivalent to the success probability given the system status at a given time instant. In addition, there are some periods of time where the system is more (region A) or less (region B) reliable than the threshold l_0. An interesting question arises:

How often the system performs with a reliability above/below the average?

In that case, the problem translates to finding the time in which the system operates in region A normalized by the total time. Also, and perhaps even more interesting than the first question:

What is the reliability of the system the x% of the time?

This implies finding l_0 such that the time in which the system operates in region A normalized by the total time is $x/100$, guaranteeing a minimum reliability level at a given amount of time. The answers to these questions are fundamental for systems that must be indeed ultra-reliable, not only in the average sense, as it may be the case of some safety applications in vehicular networks or in wireless networked control systems [15]. A step forward on that direction has been given by Angjelichinoski *et al.* [16] by not only considering the average reliability metric for design and assessment of URLLC systems, but also proposing the *Probably Correct Reliability* (PCR) metric, which allows controlling the probability that the outage probability violates a target error for a given training sample.

B. CONTRIBUTIONS AND ORGANIZATION

In this work, we take another step in characterizing the performance of ultra-reliable systems. Our contributions are four-fold: i) we overview and analyze the concepts of asymptotic/non-asymptotic error probability, and their suitability as reliability measures; ii) we highlight that the error probability with FB is a random variable (RV) in fading channels, and provide its probability distribution; iii) we discuss how to use such results for evaluating the Value-at-Risk (VaR) and Conditional VaR (CVaR) measures [17], which are fundamental for answering the motivational questions presented in Section I-A and designing ultra-reliable systems beyond the average performance; and iv) we provide numerical examples and associated discussions, which illustrate the applicability of the proposed approaches. We validate our analytical derivations via simulations.

Next, Section II overviews error probability metrics for finite (non-asymptotic) and infinite (asymptotic) blocklength; and discusses well-known risk measures. The distribution of the FB error probability and its link to the risk measures are derived and analyzed in Section III. Finally, Section IV discusses some numerical examples, and Section V concludes the paper.

Notation: $f_X(x)$ and $F_X(x)$ are the Probability Density Function (PDF) and Cumulative Distribution Function (CDF) of X, respectively. Let $\mathbb{E}(\cdot)$ denote the mathematical expectation, $\mathbb{P}(A)$ is the probability of event A, while $Q(x)$ is the Gaussian Q-function. Moreover, $X \sim \Gamma(m, 1/m)$ is a normalized gamma distributed RV with shape factor m, and

$$f_X(x) = \frac{m^m}{\Gamma(m)} x^{m-1} e^{-mx},$$
$$F_X(x) = 1 - \frac{\Gamma(m, mx)}{\Gamma(m)};$$

while $Y \sim \text{Weibull}(1/\Gamma(1+\frac{1}{\kappa}), \kappa)$ is a normalized Weibull distributed RV with parameter κ, and

$$f_Y(y) = \kappa\Gamma(1+\tfrac{1}{\kappa})\left(\Gamma(1+\tfrac{1}{\kappa})y\right)^{\kappa-1} e^{-\left(\Gamma(1+\frac{1}{\kappa})y\right)^{\kappa}},$$
$$F_Y(y) = 1 - e^{-\left(\Gamma(1+\frac{1}{\kappa})y\right)^{\kappa}}.$$

Finally, $\mathcal{O}(\cdot)$ is the big O notation.

II. PRELIMINARIES

A. ERROR PROBABILITY

Let us consider the transmission of a message over a communication link with instantaneous SINR at the destination specified by γ. The information theoretic analysis for infinite blocklength says that error free transmission is achieved as

long as $\gamma \geq e^r - 1$, where r is the transmission rate (in nats per channel use). Therefore, the error probability is

$$\epsilon_{\text{inf}}(\gamma) = \begin{cases} 1, & \gamma < e^r - 1 \\ 0, & \gamma \geq e^r - 1. \end{cases} \tag{1}$$

If the channel is quasi-static, the so-called outage probability, P_{out}, characterizes the average frequency of the above error events, thus

$$\begin{aligned} P_{\text{out}} &= \mathbb{E}_\gamma\big(\epsilon_{\text{inf}}(\gamma)\big) \\ &= \mathbb{P}\big(\gamma < e^r - 1\big) \\ &= F_\gamma\big(e^r - 1\big). \end{aligned} \tag{2}$$

However, the formulation presented in (1) may be misleading if we are restricted to use a finite number of channel uses n when communicating over a noisy channel, for which no protocol is able to achieve perfectly reliable communication. In that sense, Polyanskiy *et al.* [3] found out that the non-asymptotic error probability for an Additive White Gaussian Noise (AWGN) channel with perfect channel state information (CSI) at the receiver side[2] can be written as

$$\begin{aligned} \epsilon_{\text{fin}}(\gamma) &= Q\left(\frac{C(\gamma) - k/n + \frac{1}{2n}\ln(n) + \mathcal{O}(1)}{\sqrt{V(\gamma)/n}}\right) \\ &\approx Q\left(\frac{C(\gamma) - k/n}{\sqrt{V(\gamma)/n}}\right), \end{aligned} \tag{3}$$

where k is the message length in nats, thus, $r = k/n$, $C(\gamma) = \ln(1+\gamma)$ is the Shannon capacity and $V(\gamma) = 1 - \frac{1}{(1+\gamma)^2}$ is the channel dispersion. The approximation given in the second line of (3) holds accurate for $n \geq 100$ channel uses and has been extensively validated, e.g., in [3], [4]. The accuracy is because $\mathcal{O}(1)$ is a small constant term, while $\frac{1}{2n}\ln(n)$ vanishes quickly as n grows above 100 channel uses.[3]

Remark 1: Notice that for a given channel realization, a quasi-static fading channel becomes conditionally Gaussian on the value of γ. Then, the FB error probability is a RV that transforms RV γ according to (3).

By taking the mathematical expectation over the FB error probability RV, we attain the corresponding average error probability as

$$P_{\text{err}} = \mathbb{E}_\gamma\big(\epsilon_{\text{fin}}(\gamma)\big). \tag{4}$$

Interestingly, it has been shown in [19] that quasi-static fading makes disappear the effect of the FB in (4), $P_{\text{err}} \sim P_{\text{out}}$, specially when i) the transmit rate is not very small and/or ii) there is not a very strong line of sight (LoS) component in the communication link. The intuition behind is that the dominant error event over quasi-static fading channels is that the channel is in a deep fade. Since the transmitted symbols experience all the same fading, it follows that coding is not helpful against deep fades and (4) is accurate already for small blocklength.

The reliability of a wireless system in the physical layer has been usually characterized in terms of average error performance by means of P_{out}, or recently by means of P_{err} in the case of FB analysis. Designing the system by targeting a given average error probability is commonly accepted in the literature and in the industry. However, the average error probability is not the only metric, maybe nor the more appropriate, to characterize the reliability performance of a communication system. Next we discuss how the system may be designed considering different risk measures [17] that make use of the error probability for a more detailed analysis.

B. RISK MEASURES

As highlighted in Remark 1, the non-asymptotic error probability, ϵ_{fin}, is a RV in quasi-static fading channels, thus, it can be characterized through its PDF and CDF. Such probabilistic characterization allows using some well-known risk metrics, as those discussed next, for assessing the system reliability.

- *Standard Deviation*[4]*:* This is a frequently used measure of risk since it quantifies the amount of dispersion. However the main disadvantage is that profits, as small error probabilities, and losses, as large error probabilities, have equal impact on the standard deviation. Thus, such measure does not discriminate between distributions with different probabilities of potentially large losses. In fact, the standard deviation does not provide any information on how large potential losses may be. This metric would be accurate as a risk measure in the case of data with a symmetric PDF but this is not the typical case when dealing with error probability distributions.
- *Value-at-Risk (VaR):* It is defined as the worst loss over a target horizon within a given level of confidence [20], such that for $0 < \alpha \leq 1$:

$$\begin{aligned} \text{VaR}_{1-\alpha} &= \inf_\tau\{\tau : \mathbb{P}(\epsilon \leq \tau) \geq 1 - \alpha\} \\ &= F_\epsilon^{-1}(1 - \alpha). \end{aligned} \tag{5}$$

  Thus, $\text{VaR}_{1-\alpha}$ is the maximum error probability in the system the $(1-\alpha)\%$ of the time.
- *Conditional VaR (CVaR) or Expected Shortfall:* Although more directly related to risks than the standard deviation, the concept of VaR still suffers from some inconsistencies [17, Ch. 10]. For example, a given error probability has a certain chance to be exceeded, but if exceeded, what is the typical loss/error probability incurred? CVaR exactly answers this question

[2]Notice that perfect CSI is an ideal assumption that does not hold in practice. However, the performance under imperfect CSI can be approximated in some scenarios by that of a system under perfect CSI but with reduced SINR [18]. In these cases, (3) can be evaluated using such reduced SINR. Consequently, the theoretical results derived in this paper can be easily extended for taking into account imperfect CSI.

[3]Although in this work we use the simplified approximation given in the second line of (3), our analytical derivations can be straightforwardly extended for the case of considering also the term $\frac{1}{2n}\ln(n)$. Moreover, we would like to highlight that other non-asymptotic bounds, which could be more accurate in some scenarios, exist in the literature (check for instance [5] and references therein) but theoretical analysis departing from them are cumbersome. Therefore, we focus our efforts on using the normal approximation in (3).

[4]This is closely related with the so-called *volatility*, which is the standard deviation of the logarithmic returns [17, Ch. 10].

by characterizing the expected loss in the right tail of the distribution given a particular threshold has been crossed, thus, measuring the risky realizations. Formally speaking, CVaR is given by [20]

$$\begin{aligned}\mathrm{CVaR}_{1-\alpha} &= \mathbb{E}\big(\epsilon \big| \epsilon > \mathrm{VaR}_{1-\alpha}\big)\\ &= \frac{1}{\alpha}\int_0^{\alpha} \mathrm{VaR}_{1-\tau}\mathrm{d}\tau\\ &\overset{(a)}{=} \frac{1}{\alpha}\int_0^{\alpha} F_{\epsilon}^{-1}(1-\tau)\mathrm{d}\tau, \end{aligned} \tag{6}$$

where (a) comes from using (5).

Remark 2: The latter two metrics complement each other, thus, characterizing the risks of error much better than only relying on average values.

In the next section we attain the distribution of the probability of error in the FB regime for the case of a quasi-static fading channel, which is required in order to numerically evaluate the above risk metrics.

III. DISTRIBUTION OF THE ERROR PROBABILITY

Notice that the CDF of ϵ_{fin} can be written as

$$\begin{aligned} F_{\epsilon}(x) &= \mathbb{P}(\epsilon_{\mathrm{fin}}(\gamma) < x)\\ &\overset{(a)}{=} \mathbb{P}(\gamma > \epsilon_{\mathrm{fin}}^{-1}(x))\\ &= 1 - F_{\gamma}(\epsilon_{\mathrm{fin}}^{-1}(x)), \end{aligned} \tag{7}$$

where $\epsilon_{\mathrm{fin}}^{-1}(x)$ is the inverse function of $\epsilon_{\mathrm{fin}}(\gamma)$, and the inequality change in (a) is because their decreasing monotonicity. Notice that $\epsilon_{\mathrm{fin}}^{-1}(x)$ already poses a challenge because of the complicated dependence between ϵ_{fin} and γ according to (3). Still, we found very recently in [21] a simple and fast iterative procedure to obtain γ given ϵ_{fin}. Therein we presented (3) as a fixed point iteration equation of γ, as follows

$$\gamma^{(t)} = e^{r+\sqrt{\frac{V\left(\gamma^{(t-1)}\right)}{n}}Q^{-1}(\epsilon_{\mathrm{fin}})} - 1, \tag{8}$$

where t is the iteration index. We proposed using $\gamma^{(0)} = \infty$ since that conduces to $V\left(\gamma^{(0)}\right) = 1$, which is appropriate in most of the scenarios since $V(\gamma)$ already approaches 1 for not too small γ values.

Remark 3: We proved analytically in [21] that there is only one solution for (8) and the iterative procedure always converges. In the Appendix we provide the proof adapted to our notation here for completeness.

Figure 2 illustrates the fast convergence of the iterative procedure by using $\gamma_{\triangle} = 10^{-2}$, which is the stopping criterion for (8) such that $\left|\gamma^{(t)} - \gamma^{(t-1)}\right| < \gamma_{\triangle}$ is satisfied in the final solution for γ. As can be seen in the figure, five iterations are typically enough. Moreover, in Figure 2 we set $k = 25$ nats (36 bits), while for greater values of k the convergence is even better since the rate increases and the corresponding γ is greater, thus, the initial guess $V\left(\gamma^{(0)}\right)$ is closer to the final solution.

Then, we can write the inverse function $\epsilon_{\mathrm{fin}}^{-1}(x)$ as

$$\epsilon_{\mathrm{fin}}^{-1}(x) = \lim_{t\to\infty} g^{(t)}(e^{r+\frac{1}{\sqrt{n}}Q^{-1}(x)} - 1, x), \tag{9}$$

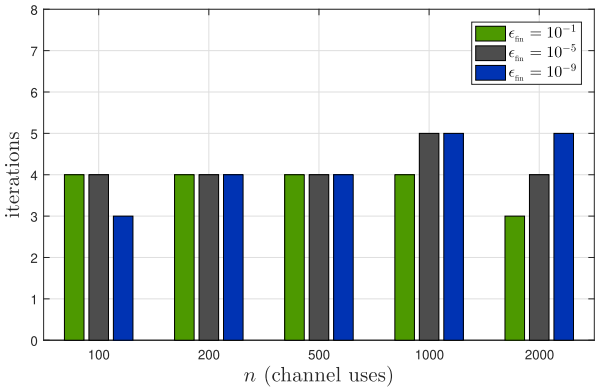

FIGURE 2. Required number of iterations for (8) as a function of n for $k = 25$ nats, $\epsilon_{\mathrm{fin}} \in \{10^{-1}, 10^{-5}, 10^{-9}\}$ and $\gamma_{\triangle} = 10^{-2}$.

where $g^{(t)}(\cdot,\cdot)$ denotes a t-times self-composition operation of

$$g(y,z) = e^{r+\sqrt{\frac{V(y)}{n}}Q^{-1}(z)} - 1 \tag{10}$$

inside its first argument, such that

$$g^{(t)}(y,z) = \underbrace{g(g(\cdots g}_{t+1}(y,z),\cdots z),z). \tag{11}$$

The starting value $e^{r+\frac{1}{\sqrt{n}}Q^{-1}(x)} - 1$ in (9) comes from setting $V(y) = 1$ in (10) for fast convergence, as commented before. Since $t = 5$ already provides a very tight approximation for (9) even in tough scenarios [21], e.g., very low data rate, it is safe to use (9) with $t \geq 5$. Therefore,

$$F_{\epsilon}(x) = 1 - \lim_{t\to\infty} F_{\gamma}\left(g^{(t)}(e^{r+\frac{1}{\sqrt{n}}Q^{-1}(x)} - 1, x)\right), \tag{12}$$

$$\approx 1 - F_{\gamma}\left(g^{(t)}(e^{r+\frac{1}{\sqrt{n}}Q^{-1}(x)} - 1, x)\right),\ t \geq 5. \tag{13}$$

Now we proceed to find the PDF of ϵ_{fin} as follows

$$f_{\epsilon}(x) = f_{\gamma}(\epsilon_{\mathrm{fin}}^{-1}(x))\left|\frac{d}{dx}\epsilon_{\mathrm{fin}}^{-1}(x)\right|. \tag{14}$$

By using (8) and setting $h(x) = \epsilon_{\mathrm{fin}}^{-1}(x)$, we obtain

$$h(x) = e^{r+\sqrt{\frac{V(h(x))}{n}}Q^{-1}(x)} - 1, \tag{15}$$

while taking the derivative at both sides leads to

$$\begin{aligned}\frac{d}{dx}h(x) &\overset{(a)}{=} \frac{h(x)+1}{\sqrt{n}}\frac{d}{dx}\sqrt{V(h(x))}Q^{-1}(x)\\ &\overset{(b)}{=} \frac{h(x)+1}{\sqrt{n}}\left[\frac{Q^{-1}(x)\frac{d}{dx}h(x)}{(1+h(x))^3\sqrt{V(h(x))}} + \right.\\ &\quad \left. -\frac{\sqrt{2\pi V(h(x))}}{e^{-\frac{1}{2}Q^{-1}(x)^2}}\right], \end{aligned} \tag{16}$$

where (a) comes from using (15) to write

$$e^{r+\sqrt{\frac{V(h(x))}{n}}Q^{-1}(x)} = h(x) + 1,$$

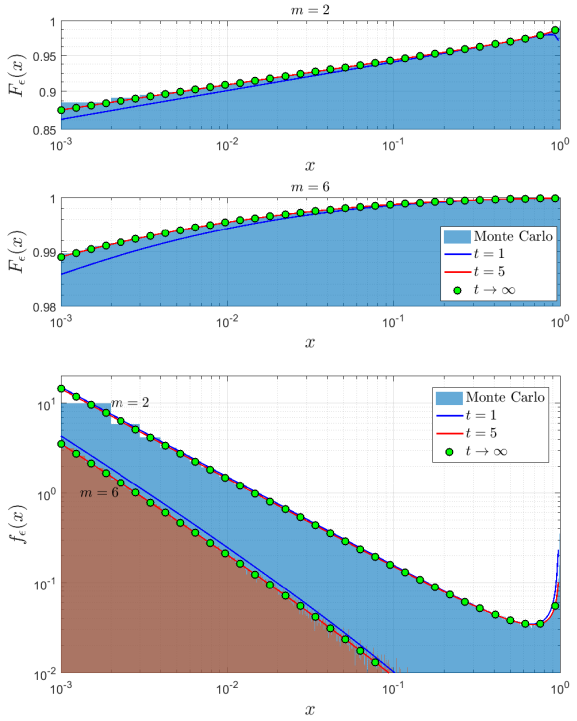

FIGURE 3. Analytical and Simulated CDF (top) and PDF (bottom) of the error probability at FB for $\gamma \sim \Gamma(m, 1/m)$. We set $n = 200$ channel uses and $k = 25$ nats.

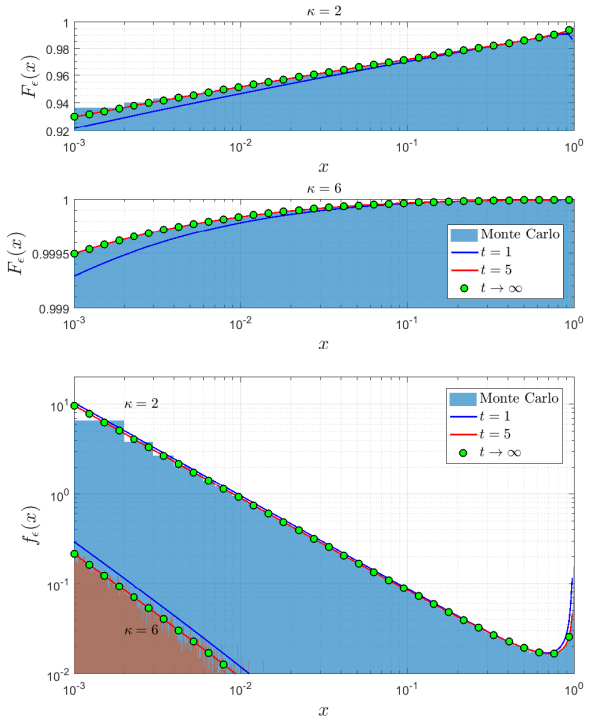

FIGURE 4. Analytical and Simulated CDF (top) and PDF (bottom) of the error probability at FB for $\gamma \sim \text{Weibull}(1/\Gamma(1+\frac{1}{\kappa}), \kappa)$. We set $n = 200$ channel uses and $k = 25$ nats.

while (b) comes from applying the rule for the derivative of a product of functions and using

$$\frac{d}{dx}Q^{-1}(x) = \frac{1}{\frac{d}{dx}Q(x)|_{x=Q^{-1}(x)}}$$

and

$$\frac{d}{dx}Q(x) = -\frac{1}{\sqrt{2\pi}}e^{-\frac{x^2}{2}}.$$

Now, we can obtain the derivative by isolating $\frac{d}{dx}h(x)$ in (16), which conduces to

$$\frac{d}{dx}h(x) = \frac{\sqrt{2\pi V(h(x))}\big(1+h(x)\big)e^{\frac{1}{2}Q^{-1}(x)^2}}{\frac{Q^{-1}(x)}{(1+h(x))^2\sqrt{V(h(x))}} - \sqrt{n}}. \tag{17}$$

Substituting (17) into (14) along with (9), yields (18), as shown at the bottom of the next page, which we can accurately approximate with $t \geq 5$ as in (13).

Remark 4: It is worth highlighting that the notion of reliability implies a success probability, thus averaging is eventually required. However, the less you average, the less information you lose. Notice that for calculating ϵ_{fin} the average is over all the error events when operating with certain γ and finding $f_{\epsilon_{\text{fin}}}(x)$ does not require further averaging, while for computing P_{err} in (4), averaging over all possible channel realizations is also required and consequently some information is lost.

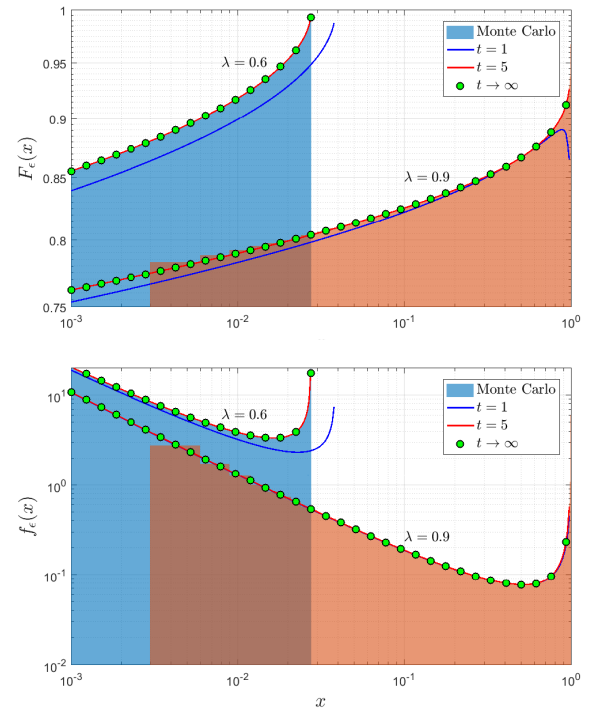

FIGURE 5. Analytical and Simulated CDF (top) and PDF (below) of the error probability at FB for γ distributed according to (19) and (20). We set $n = 200$ channel uses and $k = 25$ nats.

A. VALIDATION BY SIMULATIONS

Figures 3, 4 and 5 validate the analytical expressions of the CDF and PDF of the error probability at FB, which were obtained in (13) and (18) with finite t, respectively.

We consider three different distributions for γ, all of which are normalized such that $\mathbb{E}(\gamma) = 1$:

- Figure 3: γ is a Gamma RV, which is representative of a scenario with Nakagami-m quasi-static fading with parameter m, usually suitable for modeling line-of-sight and/or multipath communications [22];
- Figure 4: γ is a Weibull RV, which may correspond to Weibull fading with parameter κ, and it is often used for describing the fading induced by multipath propagation in indoor radio systems [23];
- Figure 5: γ is distributed with PDF and CDF given by

$$f_\gamma(x) = \frac{1}{\pi\sqrt{\lambda-(1-x)^2}},\ 1-\sqrt{\lambda} \le x \le 1+\sqrt{\lambda}, \quad (19)$$

$$F_\gamma(x) = \begin{cases} 0, & 0 \le x \le 1-\sqrt{\lambda} \\ \frac{1}{2} + \frac{1}{\pi}\tan^{-1}\left(\frac{x-1}{\sqrt{\lambda-(1-x)^2}}\right), & 1-\sqrt{\lambda} < x \le 1+\sqrt{\lambda} \\ 1, & x > 1+\sqrt{\lambda}, \end{cases} \quad (20)$$

which corresponds to the power fading caused by the interference of two constant-amplitude waves in a local area [24], where we have used $\lambda = 4V_1^2V_2^2$ such that V_1 and V_2 are the amplitudes of the multipath waves. Although this distribution is more of theoretical interest [24], it allows us to test a setup considerably different than those above and investigate the precision of our formulation.

Remark 5: Notice that, in general, the distribution of γ may be not just a direct consequence of the fading characteristics but it may include other factors, e.g., signal processing effects that come from beamforming.

In the figures, it is shown the cases of $t = 1$, $t = 5$ and $t \to \infty$. The error probability distribution in the case of $t \to \infty$ can be evaluated as follows:

1) Find $\epsilon_{\text{fin}}^{-1}(x)$ ($x \in [10^{-3}, 1)$ in the figures), which can be performed by solving numerically (15) for $h(x)$, e.g., using *vpasolve* in MatLab. This is based on the fact that (15) is equivalent to the fixed point iteration equation in (8), which converges to the exact solution for $t \to \infty$;
2) Using the value of $\epsilon_{\text{fin}}^{-1}(x)$ found in Step 1), evaluate the CDF of ϵ_{fin} at x according to (7);
3) Evaluate the PDF according to (14) and using (17).

As we can see from Figures 3, 4 and 5, the approximate PDFs and CDFs for $t = 1$ are already relatively accurate.[5] This is due to the implications of the initial value chosen for γ when iterating over (8), as commented therein. Moreover, we can also see that the simulated results match very well the analytical expressions[6] for $t = 5$.

B. EVALUATION OF THE RISK METRICS

In order to evaluate the risk metrics VaR and CVaR defined in Subsection II-B, we must find the inverse of the CDF of the error probability, which can be obtained from (7) as

$$F_\epsilon^{-1}(x) = \epsilon_{\text{fin}}\left(F_\gamma^{-1}(1-x)\right), \quad (21)$$

thus, (5) and (6) transform into

$$\text{VaR}_{1-\alpha} = \epsilon_{\text{fin}}\left(F_\gamma^{-1}(\alpha)\right), \quad (22)$$

$$\begin{aligned} \text{CVaR}_{1-\alpha} &= \frac{1}{\alpha}\int_0^\alpha \epsilon_{\text{fin}}\left(F_\gamma^{-1}(\tau)\right)\mathrm{d}\tau \\ &\overset{(a)}{=} \frac{1}{\alpha}\int_{\text{VaR}_{1-\alpha}}^1 x f_\epsilon(x)\mathrm{d}x \\ &\overset{(b)}{\approx} \frac{1}{\alpha}\int_{\text{VaR}_{1-\alpha}}^{1-\xi} x f_\epsilon(x)\mathrm{d}x \quad \text{for } \xi \ll 1, \end{aligned} \quad (23)$$

respectively. Notice that $F_\gamma^{-1}(x)$ always exists since $F_\gamma(x)$ is a strictly increasing function, but it will be difficult to compute in closed-form in most of the cases. Step (a) in (23) aims at alleviating that issue for CVaR since the inversion is only required for computing the lower bound of the integral and not during all the integration as in the precedent step. However, this advantage comes with the drawback that since $f_\epsilon(x)$ is singular at $x = 1$, the integration does not converge. A workaround can be choosing an upper limit very close to 1 as shown in step (b) but at the expense of computing an approximation instead of the exact value even when $t \to \infty$.

Remark 6: According to (22), VaR metric can be computed without relying on our analytical derivations for the error probability PDF and CDF, hence, its accuracy is guaranteed which is not the case for the CVaR metric.

Since CVaR depends on an integration over $f_\epsilon(x)$, it is sensitive to the number of iterations utilized for computing (18); however, as discussed when analyzing Figures 2, 3, 4 and 5, only few iterations should be required. Now, we take

[5] Note that Monte Carlo simulation of these PDF and CDF error probability curves are computationally affordable, however more sophisticated sampling [25] and visualization techniques are needed to represent the results at very high reliability.

[6] Notice that even when for some $x-$values, the Monte Carlo -based PDFs are highly oscillating, the CDFs are not, nor are the risk metrics.

$$f_\epsilon(x) = \lim_{t\to\infty} f_\gamma\left(g^{(t)}(e^{r+\frac{1}{\sqrt{n}}Q^{-1}(x)}-1,x)\right)\frac{\sqrt{2\pi V\left(g^{(t)}(e^{r+\frac{1}{\sqrt{n}}Q^{-1}(x)}-1,x)\right)}\left(1+g^{(t)}(e^{r+\frac{1}{\sqrt{n}}Q^{-1}(x)}-1,x)\right)e^{\frac{1}{2}Q^{-1}(x)^2}}{\left|\frac{Q^{-1}(x)}{\left(1+g^{(t)}(e^{r+\frac{1}{\sqrt{n}}Q^{-1}(x)}-1,x)\right)^2\sqrt{V\left(g^{(t)}(e^{r+\frac{1}{\sqrt{n}}Q^{-1}(x)}-1,x)\right)}}-\sqrt{n}\right|} \quad (18)$$

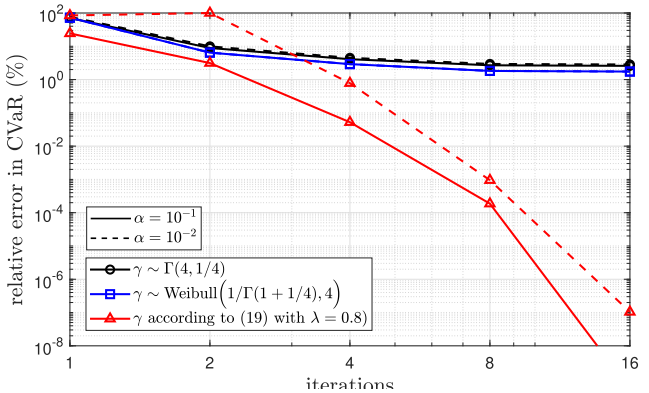

FIGURE 6. Relative error in CVaR as a function of the number of iterations for $\alpha \in \{10^{-1}, 10^{-2}\}$ and γ distributed as a Gamma RV, Weibull RV or according to (19) and (20). We set $n = 200$ channel uses, $k = 25$ nats and $\xi = 10^{-3}$.

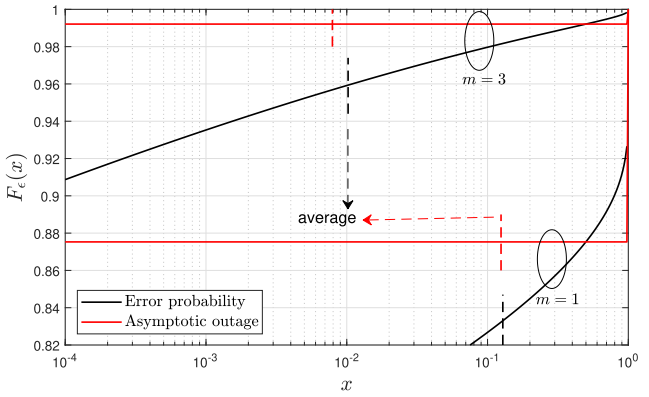

FIGURE 7. CDF of ϵ_{fin} for $\gamma \sim \Gamma(m, 1/m)$ with $m \in \{1, 3\}$.

advantage of the fact that $F_\gamma^{-1}(x)$ exists when γ is Gamma, Weibull, or according to (19), distributed for showing in Figure 6 the relative error when using (23) as a function of the number of iterations. It is observed that the accuracy increases as more iterations are utilized, specially when γ is distributed according to (19), which means that this kind of distribution is less sensitive to ξ. On the contrary, utilizing more than 4 iterations does not help significantly the accuracy of (23) because of the relative large value of ξ when γ is a Gamma or Weibull RV. In any case, a relative error around 4% can be guaranteed with at least 5 iterations. For instance, this means that if the exact CVaR is 0.01 or 0.1, using 5 iterations could lead to a CVaR estimate of 0.01 ± 0.0004 or 0.1 ± 0.004, respectively.

IV. NUMERICAL EXAMPLES

In this section, we illustrate how the previous derivations can be used to better comprehend the error probability behavior[7] of wireless systems operating with FB. Next we set $t = 5$, $k = 25$ nats, and $n = 200$ channel uses, while $\mathbb{E}(\gamma) = 1$ (0 dB) for all the SINR distributions.

A. ASYMPTOTIC VS NON-ASYMPTOTIC ERROR PROBABILITY DISTRIBUTION

Figure 7 shows the CDF of the error probability when the system operates with a Gamma distributed SINR. The curves are compared with the CDF of the asymptotic outage probability, which is a two-mass-point RV with one mass point at 0 with probability $1 - P_{\text{out}}$, and the other at 1 with probability P_{out}. Notice that the outage probability differs more from the non-asymptotic average error probability as m increases and commented in Section II-A. For example, for $m = 1$ the gap

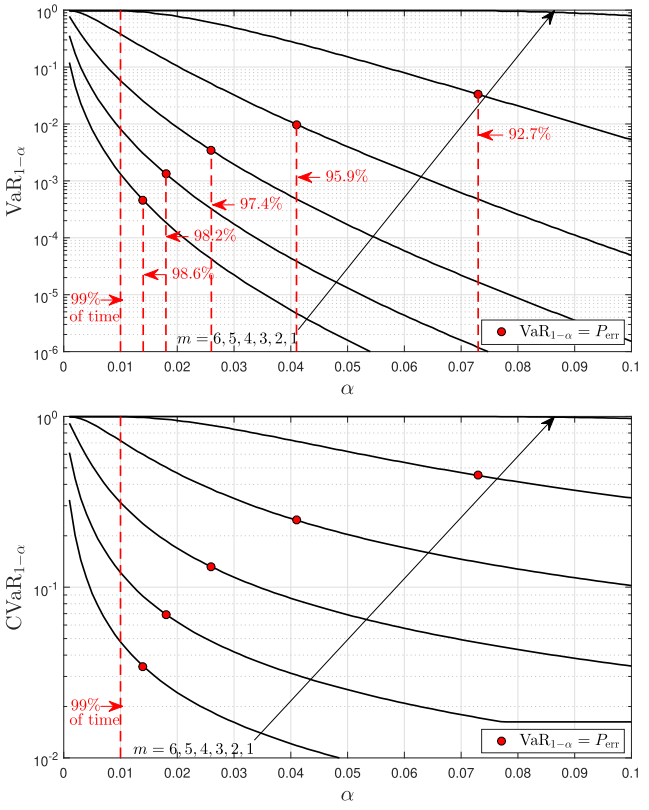

FIGURE 8. *a*) $\text{VaR}_{1-\alpha}$ (top) and *b*) $\text{CVaR}_{1-\alpha}$ (bottom) as a function of α for $\gamma \sim \Gamma(m, 1/m)$ with $m \in \{1, 2, 3, 4, 5, 6\}$.

between P_{out} and P_{err} is small since $\frac{P_{\text{err}}}{P_{\text{out}}} \approx 1.03$, but it starts increasing such that for $m = 3$ yields $\frac{P_{\text{err}}}{P_{\text{out}}} \approx 1.29$, while for $m = 6$ (not shown in Figure 7) is already considerable since $\frac{P_{\text{err}}}{P_{\text{out}}} \approx 2.65$. Thus, the asymptotic result is not adequate for analyzing the system reliability when there is strong LoS, not even in the average sense.

B. INFORMATION INSIGHTS FROM THE RISK MEASURES

In Figure 8, we show the VaR and CVaR as functions of α, which represent the maximum error probability of the system the $(1 - \alpha)\%$ of the time, and the average error once

[7]The results drawn in this section are in general with an average reliability below the typical requirements for URLLC [1]. This is necessary in order to visualize important performance trends and corroborate fundamental gaps between different reliability formulations. However, notice that all analytical results in the previous sections are valid and can be evaluated in the region of extremely small error probabilities.

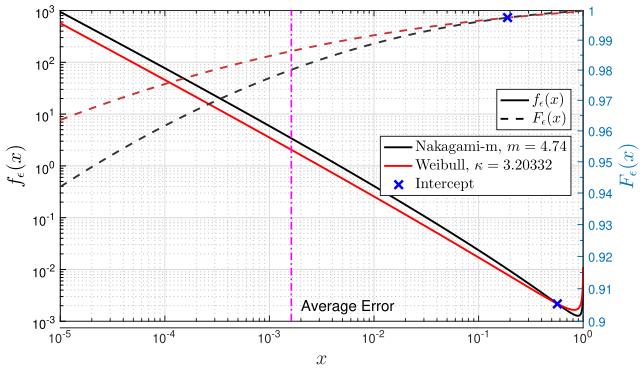

FIGURE 9. PDF and CDF of ϵ_{fin} for L1 (Nakagami-m) and L2 (Weibull).

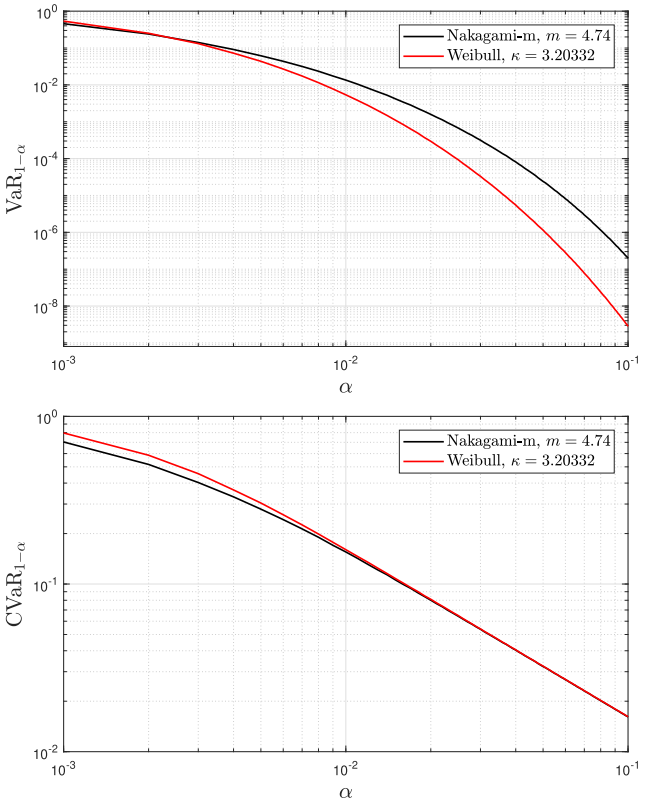

FIGURE 10. *a*) $\text{VaR}_{1-\alpha}$ (top) and *b*) $\text{CVaR}_{1-\alpha}$ (bottom) for L1 (Nakagami-m) and L2 (Weibull).

the system operates with an error probability above the VaR value, respectively. Clearly, both metrics are non-increasing functions of α. We have also marked the points for which the average error probability matches the value of $\text{VaR}_{1-\alpha}$. For instance, consider that the target average error probability is $P_{\text{err}} \approx 10^{-2}$ and that $m = 3$. In Figure 8a, using the VaR metric, we can see that an error probability below the average occurs during 95.9% of the time. Thus, the instantaneous reliability in almost 4% of the time will be certainly smaller than the one designed in the average sense. Indeed, from the same figure we can see that the error probability is larger than 0.4 during 1% of the time, certainly unacceptable for most applications. Moreover, for the same case of $m = 3$ and considering the worst 1% channel realizations (to the left of the 99% line), we can see in Figure 8b that the average error probability is 0.7, extremely high. The main message from the above analysis is that the average error probability does not provide all the information that is needed in order to fully characterize the reliability of the system.

C. A RISK-BASED COMPARATIVE EXAMPLE

Metrics like VaR and CVaR contribute to better characterize the system reliability, and reveal that it is important to include in the system design the maximum acceptable probability of average reliability violation, so that a margin in SINR or in transmission rate is adequately taken into account during the system design phase. In order to further illustrate the above analysis, let us consider two different communication links where the SINR at the destination behaves as a RV such that:

L1 $\gamma \sim \Gamma(m, 1/m)$, $m = 4.74$ (Nakagami-m);
L2 $\gamma \sim \text{Weibull}\big(1/\Gamma(1+\frac{1}{\kappa}), \kappa\big)$, $\kappa = 3.20332$.

These systems have the peculiarity that they share the same average error performance[8]: $P_{\text{err}}^{(1)} = P_{\text{err}}^{(2)} = 1.62 \times 10^{-3}$. *Are they equally reliable?* In order to answer this question, let us take a look at the distributions of the error probabilities, shown in Figure 9. Although both links share the same average error performance, their statistics are considerably different. The main conclusion from Figure 9 is that when the links operate under good channel conditions, e.g., error probabilities below 0.2, **L2** is more reliable than **L1** since the error probability CDF of the former lies completely above of that of its counterpart in that region. Thus, **L2** is operating with error probabilities below ϵ_{th}, such that $\epsilon_{\text{th}} < 0.2$, more frequently than **L1**. However, when the channel behaves poorly, with $\epsilon_{\text{fin}} > 0.2$, then **L1** outperforms **L2**. This happens around 0.3% of the time since $1 - F_\epsilon(0.2) \approx 0.003$ for both links. The y-coordinate of the intercept point of the CDF curves, y^*, delimits the fraction of time where one system outperforms the other. For a more detailed analysis, let us introduce a comparison of the risk metrics for these scenarios as depicted in Figure 10, while Table 1gives a collection of VaR and CVaR values related to the performance of both links, where the values in bold are those corresponding to the best performance. Notice that the VaR of **L2** is the best for $\alpha \in [0.01, 0.1]$; in fact, according to Figure 9 that happens always as long as $\alpha < 1 - y^*$. Meanwhile, the CVaR of **L1** turned out to be the best for all the tested values of α, however notice that the gain in VaR of **L2** with respect to **L1** is much larger than the corresponding loss in CVaR for $\alpha > 0.01$. Let us interpret some specific results. According to Table I, 99% of the time, the maximum error probability of the system is 1.34×10^{-2} for **L1** and 5.38×10^{-3} for **L2**, a considerable advantage in favor of **L2**; while for the 1% worst channel realizations, when the SINR is very low, then the errors happen with probabilities 0.1559 and 0.1597, which are basically

[8]This is for $n = 200$ channel uses and $k = 25$ nats.

TABLE 1. Comparison between communication links 1 and 2 in terms of some risk measures.

Comm.	$\alpha = 0.1$		$\alpha = 0.05$		$\alpha = 0.01$		$\alpha = 0.001$	
Link	VaR	CVaR	VaR	CVaR	VaR	CVaR	VaR	CVaR
L1	1.99×10^{-7}	$\mathbf{1.62 \times 10^{-2}}$	2.42×10^{-5}	$\mathbf{3.24 \times 10^{-2}}$	1.34×10^{-2}	**0.1559**	**0.4530**	**0.7001**
L2	$\mathbf{2.84 \times 10^{-9}}$	1.62×10^{-2}	$\mathbf{1.13 \times 10^{-6}}$	3.24×10^{-2}	$\mathbf{5.38 \times 10^{-3}}$	0.1597	0.5419	0.7995

the same. We can even evaluate the average error probability during 99% of the time by calculating $\frac{1}{1-\alpha}\int_0^{\text{VaR}_{1-\alpha}} x f_\epsilon(x)\mathrm{d}x$ with $\alpha = 0.01$, which leads to 6.2×10^{-5} and 2.3×10^{-5} for **L1** and **L2**, respectively. In fact, using those values we are able to go back to the average error probability if we evaluate $P_{\text{err}}^{(1)} = 6.2 \times 10^{-5} \times 0.99 + 0.1559 \times 0.01$ and $P_{\text{err}}^{(2)} = 2.3 \times 10^{-5} \times 0.99 + 0.1597 \times 0.01$, and notice that both results match the value considered at the beginning of this paragraph: $P_{\text{err}} = 1.62 \times 10^{-3}$.

Therefore, for a single (or few) message transmission where it is more likely operating in the region of good channel performance, **L2** is considerably more reliable than **L1**, although the average performance is the same. Thus, the above results show the importance of the proposed reliability analysis as well as the fact that different channel distributions may lead to considerable different reliability behaviors, even if the channels behave similarly in the average sense.

V. CONCLUSION

We provided accurate analytical approximations for the distribution of the non-asymptotic error probability in wireless communication system with fixed transmit rate. We evaluate well-known risk measures that use such statistics to provide more insights on the reliability performance of the system. Numerical methods corroborated our findings, while we discussed two examples that evidence the fact that relying only on the average error performance may be far from sufficient for a definitive characterization of the system reliability. As a future work, we plan to propose and analyze efficient resource scheduling strategies for URLLC with risk-based reliability guarantees.

APPENDIX

We next reproduce and extend our proof in [21, App. C] while adapting it to the notation utilized in this paper. We require to solve $f(\gamma) = q(\gamma) - \gamma = 0$, where

$$q(\gamma) = q_1 q_2^{\sqrt{V(\gamma)}} - 1,$$

$q_1 = e^r \geq 1$ since $r \geq 0$, and $q_2 = e^{\frac{1}{\sqrt{n}}Q^{-1}(\epsilon_{\text{fin}})}$. Note that $f(\gamma)$ is continuous, while $f(0) = q_1 - 1 \geq 0$ and $\lim_{\gamma\to\infty} f(\gamma) = -\infty$, thus there is at least one γ such that $f(\gamma) = 0$. Then, we can argue as follows

- Case I: $\epsilon_{\text{fin}} \geq 0.5$
  For this case $Q^{-1}(\epsilon_{\text{fin}}) \leq 0$, thus $q(\gamma)$ is non-increasing and γ is increasing and there is only one solution to $q(\gamma) = \gamma$.
- Case II: $\epsilon_{\text{fin}} < 0.5$
  Now $Q^{-1}(\epsilon_{\text{th}}) > 0$, thus $q(\gamma)$ is also increasing. Taking its derivatives we have

$$q'(\gamma) = \frac{q_1 q_2^{\sqrt{V(\gamma)}} \ln(q_2)}{(1+\gamma)^3 V(\gamma)}, \tag{24}$$

$$q''(\gamma) = -\frac{\ln(q_2) q_1 q_2^{\sqrt{V(\gamma)}}}{\sqrt{V(\gamma)}(1+\gamma)^2}\Big[\frac{1}{(1+\gamma)^2\sqrt{V(\gamma)}} + +3 - \frac{\ln(q_2)}{(1+\gamma)^2}\Big], \tag{25}$$

where $\ln(q_2) > 0$. Thus, we can claim that $g(\gamma)$ is concave if

$$\begin{aligned} \frac{1}{(1+\gamma)^2\sqrt{V(\gamma)}} + 3 &> \frac{\ln(q_2)}{(1+\gamma)^2} \\ q_2 &< e^{\frac{1}{\sqrt{V(\gamma)}}+3(1+\gamma)^2} \\ Q^{-1}(\epsilon_{\text{fin}}) &< \sqrt{n}\big(\tfrac{1}{\sqrt{V(\gamma)}} + 3(1+\gamma)^2\big) \\ \epsilon_{\text{fin}} &> Q\Big(\sqrt{n}\big(\tfrac{1}{\sqrt{V(\gamma)}}+3(1+\gamma)^2\big)\Big), \end{aligned} \tag{26}$$

where the right side is maximized for the minimum value of $\sqrt{n}\big(\frac{1}{\sqrt{V(\gamma)}} + 3(1+\gamma)^2\big)$. Setting $n = 100$, which is the minimum value for which all the analyses are valid, and $\gamma = 0.1655$, which minimizes the remaining terms, we reach $\epsilon_{\text{fin}} > Q(46.6364) \approx 4.4 \times 10^{-475}$. Evidently, that requirement is met for any setup of practical interest. Thus, $q(\gamma)$ is increasing and concave and since $q(0) > 0$, which is the starting point of line γ, we conclude that they intersect at one point only. Therefore, the solution is unique.

Thus, we can say that the unique solution of $f(\gamma) = 0$ is a fixed point of

$$e^{r+\sqrt{\frac{V(\gamma)}{n}}Q^{-1}(\epsilon_{\text{fin}})} - 1.$$

Based on the Fixed Point Theory [26], if $|q'(\gamma)| < 1$, the fixed point iteration in (8) will converge to the solution. Using (24) and performing some algebraic transformations, yields

$$|q'(\gamma)| = \left|\frac{q_1 q_2^{\sqrt{V(\gamma)}}\ln(q_2)}{(1+\gamma)^3\sqrt{V(\gamma)}}\right| \overset{(a)}{=} \frac{e^r e^{\sqrt{\frac{V(\gamma)}{n}}Q^{-1}(\epsilon_{\text{fin}})}\frac{|Q^{-1}(\epsilon_{\text{fin}})|}{\sqrt{n}}}{(1+\gamma)^3\sqrt{V(\gamma)}}$$

$$\overset{(b)}{=} \frac{e^r e^{\ln(1+\gamma)-r} \frac{|\ln(1+\gamma)-r|}{\sqrt{V(\gamma)}}}{(1+\gamma)^3\sqrt{V(\gamma)}} \overset{(c)}{=} \frac{|\ln(1+\gamma)-r|}{\gamma(\gamma+2)}, \quad (27)$$

where (a) and (b) come from using the expressions of q_1 and q_2, and

$$Q^{-1}(\epsilon_{\text{fin}}) = \frac{\ln(1+\gamma)-r}{\sqrt{\frac{V(\gamma)}{n}}}$$

(see (3)), respectively; while (c) is attained after substituting $V(\gamma) = 1 - \frac{1}{(1+\gamma)^2}$ followed by some simplifications. Now, for $\epsilon_{\text{fin}} \leq 0.5$ we have that $\ln(1+\gamma) \geq r$, thus

$$|q'(\gamma)| < \frac{\ln(1+\gamma)}{\gamma(\gamma+2)} < 1, \ \forall \gamma \geq 0, \quad (28)$$

while for $\epsilon_{\text{fin}} > 0.5$ we have that

$$|q'(\gamma)| = \frac{r - \ln(1+\gamma)}{\gamma(\gamma+2)}, \quad (29)$$

which is smaller than 1 as long as $r < \gamma(\gamma+2) + \ln(1+\gamma)$. Interestingly, utilizing this rate bound we attain

$$\epsilon_{\text{fin}} < Q\Big(-\sqrt{n}\sqrt{1 + \frac{1}{\gamma^2(\gamma+2)^2}}\Big),$$

which independently of γ is very close to 1 for $n \geq 100$ channel uses. Consequently $|q'(\gamma)| < 1$ holds also for this case. Therefore, and from Banach's fixed point theorem [26], the (at least) linear convergence of a Fixed-point iteration algorithm is guaranteed provided any initial point $\gamma^{(0)}$.

REFERENCES

[1] D. Soldani, Y. J. Guo, B. Barani, P. Mogensen, C.-L. I, and S. K. Das, "5G for ultra-reliable low-latency communications," *IEEE Netw.*, vol. 32, no. 2, pp. 6–7, Mar. 2018.
[2] G. Durisi, T. Koch, and P. Popovski, "Toward massive, ultrareliable, and low-latency wireless communication with short packets," *Proc. IEEE*, vol. 104, no. 9, pp. 1711–1726, Sep. 2016.
[3] Y. Polyanskiy, H. V. Poor, and S. Verdu, "Channel coding rate in the finite blocklength regime," *IEEE Trans. Inf. Theory*, vol. 56, no. 5, pp. 2307–2359, May 2010.
[4] W. Yang, G. Durisi, T. Koch, and Y. Polyanskiy, "Quasi-static multiple-antenna fading channels at finite blocklength," *IEEE Trans. Inf. Theory*, vol. 60, no. 7, pp. 4232–4265, Jul. 2014.
[5] M. C. Coşkun, G. Durisi, T. Jerkovits, G. Liva, W. Ryan, B. Stein, and F. Steiner, "Efficient error-correcting codes in the short blocklength regime," *Phys. Commun.*, vol. 34, pp. 66–79, Jun. 2019.
[6] H. Shariatmadari, S. Iraji, and R. Jantti, "Analysis of transmission methods for ultra-reliable communications," in *Proc. IEEE 26th Annu. Int. Symp. Pers., Indoor, Mobile Radio Commun. (PIMRC)*, Aug. 2015, pp. 2303–2308.
[7] J. Ostman, G. Durisi, E. G. Strom, M. C. Coskun, and G. Liva, "Short packets over block-memoryless fading channels: Pilot-assisted or noncoherent transmission?" *IEEE Trans. Commun.*, vol. 67, no. 2, pp. 1521–1536, Feb. 2019.
[8] O. L. A. Lopez, H. Alves, R. D. Souza, and E. M. G. Fernandez, "Ultra-reliable short-packet communications with wireless energy transfer," *IEEE Signal Process. Lett.*, vol. 24, no. 4, pp. 387–391, Apr. 2017.
[9] Y. Gu, H. Chen, Y. Li, and B. Vucetic, "Ultra-reliable short-packet communications: Half-duplex or full-duplex relaying?" *IEEE Wireless Commun. Lett.*, vol. 7, no. 3, pp. 348–351, Jun. 2018.
[10] G. C. Ferrante, J. Ostman, G. Durisi, and K. Kittichokechai, "Pilot-assisted short-packet transmission over multiantenna fading channels: A 5G case study," in *Proc. 52nd Annu. Conf. Inf. Sci. Syst. (CISS)*, Mar. 2018, pp. 1–6.
[11] O. L. Alcaraz Lopez, H. Alves, and M. Latva-Aho, "Rate control under finite blocklength for downlink cellular networks with reliability constraints," in *Proc. 15th Int. Symp. Wireless Commun. Syst. (ISWCS)*, Aug. 2018, pp. 1–6.
[12] O. L. A. Lopez, H. Alves, and M. Latva-Aho, "Distributed rate control in downlink NOMA networks with reliability constraints," *IEEE Trans. Wireless Commun.*, vol. 18, no. 11, pp. 5410–5423, Nov. 2019.
[13] M. Bennis, M. Debbah, and H. V. Poor, "Ultrareliable and low-latency wireless communication: Tail, risk, and scale," *Proc. IEEE*, vol. 106, no. 10, pp. 1834–1853, Oct. 2018.
[14] T. K. Vu, M. Bennis, M. Debbah, M. Latva-aho, and C. S. Hong, "Ultra-reliable communication in 5G mmWave networks: A risk-sensitive approach," *IEEE Commun. Lett.*, vol. 22, no. 4, pp. 708–711, Apr. 2018.
[15] P. Park, S. C. Ergen, C. Fischione, C. Lu, and K. H. Johansson, "Wireless network design for control systems: A survey," *IEEE Commun. Surveys Tuts.*, vol. 20, no. 2, pp. 978–1013, 2nd Quart., 2018.
[16] M. Angjelichinoski, K. F. Trillingsgaard, and P. Popovski, "A statistical learning approach to ultra-reliable low latency communication," *IEEE Trans. Commun.*, vol. 67, no. 7, pp. 5153–5166, Jul. 2019.
[17] J.-P. Bouchaud and M. Potters, *Theory of Financial Risk and Derivative Pricing*. Cambridge, U.K.: Cambridge Univ. Press, 2009.
[18] O. L. Alcaraz Lopez, E. M. G. Fernandez, R. D. Souza, and H. Alves, "Ultra-reliable cooperative short-packet communications with wireless energy transfer," *IEEE Sensors J.*, vol. 18, no. 5, pp. 2161–2177, Mar. 2018.
[19] P. Mary, J. M. Gorce, A. Unsal, and H. V. Poor, "Finite blocklength information theory: What is the practical impact on wireless communications?" in *Proc. IEEE Globecom Workshops*, Dec. 2016, pp. 1–6.
[20] A. J. McNeil, R. Frey, and P. Embrechts, *Quantitative Risk Management: Concepts, Techniques and Tools, Revised Edition*. Princeton, NJ, USA: Princeton Univ. Press, 2015.
[21] O. L. A. López, E. M. G. Fernández, R. D. Souza, and H. Alves, "Wireless powered communications with finite battery and finite blocklength," *IEEE Trans. Commun.*, vol. 66, no. 4, pp. 1803–1816, Apr. 2018.
[22] M. K. Simon and M.-S. Alouini, *Digital Communication Over Fading Channels*, vol. 95. Hoboken, NJ, USA: Wiley, 2005.
[23] F. Babich and G. Lombardi, "Statistical analysis and characterization of the indoor propagation channel," *IEEE Trans. Commun.*, vol. 48, no. 3, pp. 455–464, Mar. 2000.
[24] G. D. Durgin, T. S. Rappaport, and D. A. de Wolf, "New analytical models and probability density functions for fading in wireless communications," *IEEE Trans. Commun.*, vol. 50, no. 6, pp. 1005–1015, Jun. 2002.
[25] R. Y. Rubinstein and D. P. Kroese, *Simulation and the Monte Carlo Method* (Wiley Series in Probability and Statistics). Hoboken, NJ, USA: Wiley, Nov. 2016. [Online]. Available: http://doi.wiley.com/10.1002/9781118631980
[26] R. P. Agarwal, M. Meehan, and D. O'Regan, *Fixed Point Theory and Applications*, vol. 141. Cambridge, U.K.: Cambridge Univ. Press, 2001.

ONEL L. ALCARAZ LÓPEZ (Member, IEEE) was born in Sancti-Spíritus, Cuba, in 1989. He received the B.Sc. (Hons.) degree in electrical engineering from the Central University of Las Villas, Cuba, in 2013, the M.Sc. degree from the Federal University of Paraná, Brazil, in 2017, and the D.Sc. degree from the University of Oulu, Finland, in 2020. From 2013 to 2015, he served as a Specialist in telematics at Cuban Telecommunications Company (ETECSA). His research interests are in wireless communications, specifically in ultra-reliable, low-latency communications for future networks, energy harvesting setups, and efficient access techniques for massive machine-type communications. He was a collaborator of the 2016 Research Award given by the Cuban Academy of Sciences and a Corecipient of the 2019 IEEE European Conference on Networks and Communications (EuCNC) Best Student Paper Award.

HIRLEY ALVES (Member, IEEE) received the B.Sc. and M.Sc. degrees in electrical engineering from the Federal University of Technology-Paraná (UTFPR), Brazil, in 2010 and 2011, respectively, and the dual D.Sc. degree from the University of Oulu, Oulu, Finland, and the UTFPR, in 2015. In 2017, he was an Adjunct Professor in machine-type wireless communications with the Centre for Wireless Communications (CWC), University of Oulu. In 2019, he joined the CWC, University of Oulu, as an Assistant Professor, and is currently the Head of the Machine-Type Wireless Communications Group. He is actively working on massive connectivity and ultra-reliable low latency communications for future wireless networks, 5G and 6G, full-duplex communications, and physical-layer security. He leads the URLLC activities of the 6G Flagship Program. He was a Corecipient of the 2016 Research Award from the Cuban Academy of Sciences and the 2017 IEEE International Symposium on Wireless Communications and Systems (ISWCS) Best Student Paper Award. He has been the organizer, the chair, a TPC member, and a tutorial lecturer of several renowned international conferences. He was the General Chair of the ISWCS 2019 and the Co-Chair of the First 6G Summit, Levi 2019.

RICHARD DEMO SOUZA (Senior Member, IEEE) received the D.Sc. degree in electrical engineering from the Federal University of Santa Catarina (UFSC), in 2003. From 2004 to 2016, he was with the Federal University of Technology-Paraná (UTFPR), Brazil. Since 2017, he has been with the UFSC, where he is an Associate Professor. His research interests are in the areas of wireless communications and signal processing. He was a Corecipient of the 2014 IEEE/IFIP Wireless Days Conference Best Paper Award and the 2016 Research Award from the Cuban Academy of Sciences, and the Supervisor of the Best Ph.D. Thesis Award in Electrical Engineering, Brazil, in 2014.

MATTI LATVA-AHO (Senior Member, IEEE) received the M.Sc., Lic.Tech., and Dr.Tech. (Hons.) degrees in electrical engineering from the University of Oulu, Oulu, Finland, in 1992, 1996, and 1998, respectively. From 1992 to 1993, he was a Research Engineer with Nokia Mobile Phones, Oulu, after which he joined the Centre for Wireless Communications (CWC), University of Oulu. He was the Director of the CWC, from 1998 to 2006, and the Head of the Department for Communication Engineering, until August 2014. He has been serving as an Academy of Finland Professor, since 2017. He is currently a Professor of digital transmission techniques with the University of Oulu. His research interests are related to mobile communication systems, and his group currently focuses on 5G and beyond systems research.